

Article

Not peer-reviewed version

---

# Synergistic Improvement of Mechanical and Corrosion Properties in TiN PVD-Coated Tool Steels via PAN Pre-treatment

---

[Mahdi Dadfar](#)<sup>\*</sup>, Hamid Reza Khandan Pour, Tiberio Sanvito

Posted Date: 29 September 2023

doi: 10.20944/preprints202309.2019.v1

Keywords: nitriding; physical vapour deposition (PVD); mechanical properties testing; corrosion; scratch hardness



Preprints.org is a free multidiscipline platform providing preprint service that is dedicated to making early versions of research outputs permanently available and citable. Preprints posted at Preprints.org appear in Web of Science, Crossref, Google Scholar, Scilit, Europe PMC.

Copyright: This is an open access article distributed under the Creative Commons Attribution License which permits unrestricted use, distribution, and reproduction in any medium, provided the original work is properly cited.

## Article

# Synergistic Improvement of Mechanical and Corrosion Properties in TiN PVD-Coated Tool Steels via PAN Pre-Treatment

M. Dadfar <sup>a,1</sup>, H. R. Khandan Pour <sup>a,b</sup> and T. Sanvito <sup>a</sup>

<sup>a</sup> R&D group, CRT S.r.l., Viale Primo Maggio, 19, 20014 Nerviano (MI), Italy

<sup>b</sup> Department of materials engineering, Polytechnic University of Milan, Milan, Italy

**Abstract:** Chemical and mechanical properties of plasma-assisted nitrided (PAN), TiN cathodic arc coated, and PAN with TiN coated samples were thoroughly evaluated on tool steel samples of 1.2379. The evaluation involved SEM, nano-indentation, profilometer, micro scratch, and corrosion tests. The results revealed that PAN treatment alters the roughness of the surface, while it has minimal impact on the coefficient of friction. However, it increases the substrate's hardness, making it twice as hard and three times more resilient against scratch tests, along with improved corrosion resistance. TiN-coated samples are four times harder than untreated ones, but they exhibit a higher elastic modulus (E), leading to a lower H/E index. The most promising results were obtained with PAN+TiN treatment, combining high hardness (H) with lower E, resulting in a high H/E index, a crucial criterion for wear resistance. These samples also demonstrated superior scratch hardness and corrosion resistance, despite being thinner and rougher.

**Keywords:** nitriding; physical vapour deposition (PVD); mechanical properties testing; corrosion; scratch hardness

TiN coatings are known for their high hardness, which contributes to their excellent wear resistance and low friction properties. They also provide good corrosion resistance, protecting the underlying substrate from chemical attacks and oxidation [1–4]. Nevertheless, TiN coatings exhibit brittleness, making them prone to cracking or delamination under certain mechanical stresses. Furthermore, achieving thicker TiN on a deformable substrate, the intrinsic stresses also rise accordingly. Consequently, thick and hard coatings are unsuitable for providing tribological protection to soft substrate materials [4].

Nitriding can significantly improve the wear resistance of PVD coatings by forming a hard and wear-resistant nitrided layer on the surface. This layer can reduce friction and wear, thereby increasing the longevity of the PVD coating. Moreover, nitriding can increase the adhesion of the PVD coating to the substrate by forming a metallurgical bond between the coating and the substrate. This can enhance the coating's resistance to delamination or spallation. Nitriding can also improve the fatigue resistance of PVD coatings by increasing the surface hardness and reducing the coefficient of friction [5].

Researchers [6,7] have examined the positive impact of nitriding steel prior to PVD coating, leading to reduced wear on TiN under such conditions. It is widely recognized that the wear resistance of a coated tool significantly relies on the adhesion of the coating to the substrate. K. Hock and et al. [8] concluded that by prenitriding and using a gradient interlayer system during deposition, the adhesion can be enhanced. The tool steels exhibit increased resistance to metal cutting and forming as a result of the formation of a duplex layer tailored for specific applications. They found that while the contact fatigue limit is strongly influenced by the nitrided case, the wear caused by sliding and abrasion is reduced by the hardcoating, which is particularly advantageous for machine

<sup>1</sup> Corresponding author: [mdadfar2001@gmail.com](mailto:mdadfar2001@gmail.com)

components that experience greater levels of slippage. Therefore, the characteristics acquired through the combination of nitriding and hardcoating enable functional sharing among the core material, the hardened case, and the surface, which is of special interest for application in complex stressed parts.

This study aims to provide a comprehensive analysis of arc PVD of TiN coatings, elucidating their strengths and weaknesses. Although TiN coatings have gained recognition for their exceptional hardness, wear resistance, and corrosion resistance, they also have some limitations. This paper investigates the potential of PAN as a pre-surface modification technique to overcome the drawbacks of TiN coatings, while simultaneously saving time, energy, and costs, thanks to the advanced available machines.

A heat treatable high carbon-high chromium disk-shaped tool steel (1.2379) was chosen as the substrate material. Topography and surface roughness of the samples were evaluated before and after each treatment using a 3D optical profilometer available at CRT. The profilometer was integrated into an advanced PB1000 mechanical tester machine, equipped with additional modules for nano-indentation, micro-scratch, and friction analysis, enabling comprehensive characterization of the mechanical properties of thin layers.

For the present study, four types of samples were investigated: untreated, PAN-treated, TiN-coated, and a combination of PAN and TiN coated. Samples were mounted in one-fold (1R) and two-fold (2R) rotations to compare their properties against the untreated sample in terms of hardness, roughness, elastic modulus, friction coefficient, and corrosion resistance. Table 1 presents the key parameters for both PAN and TiN coating processes.

**Table 1.** Coating parameters of new and old PVD machines.

Treatment	Temperature (°C)	Pressure (mbar)	Cathode or Plasma Current (A)	Gas ratio (N <sub>2</sub> /H <sub>2</sub> )	Duration (h)	Bias (V)
PAN	<500	8×10 <sup>-3</sup>	80	30/70	3	-50
TiN	<500	2×10 <sup>-2</sup>	150	100/0	1	-40

Microstructure and surface morphology were observed by Optical Microscopy (OM) and SEM while nano-hardness, micro-scratch, and friction coefficient tests were conducted using PB1000 mechanical tester machine. Nano-hardness calculations were determined with the fixed penetration force of 50 mN. The hardness values are an average of at least five measurements.

The corrosion resistances of untreated, PAN, TiN, and PAN+TiN samples were assessed using potentiostatic (PS) experiments conducted with a Gamry instrument. The experiment utilized a standard three-electrode setup consisting of a platinum counter electrode, a saturated Ag/AgCl electrode. All measurements were referenced to Ag/AgCl in 0.5% NaCl solution stabilized for a duration of 30 minutes.

Adhesion properties were evaluated using a micro scratch tester equipped with a diamond indenter featuring a spherical point with a tip radius of 0.1 mm. The critical load for complete delamination of the coating from the substrate, known as LC3, was identified.

Figure 1 illustrates the profilometry results obtained from the top view of various samples. The untreated sample exhibits the lowest surface roughness, as it was meticulously finished up to 1µm using diamond paste. However, the surface roughness increases significantly to more than five times the original surface roughness due to the intense bombardment of Argon ions during the PAN treatment.

Continuing the same trend after TiN coating application highlights the importance of the previous treatments on surface roughness. Surprisingly, the TiN coating not only fails to improve the roughness but actually exacerbates the surface quality. The data presented in Table 2 confirms that this effect is less pronounced in the two-fold rotation samples.

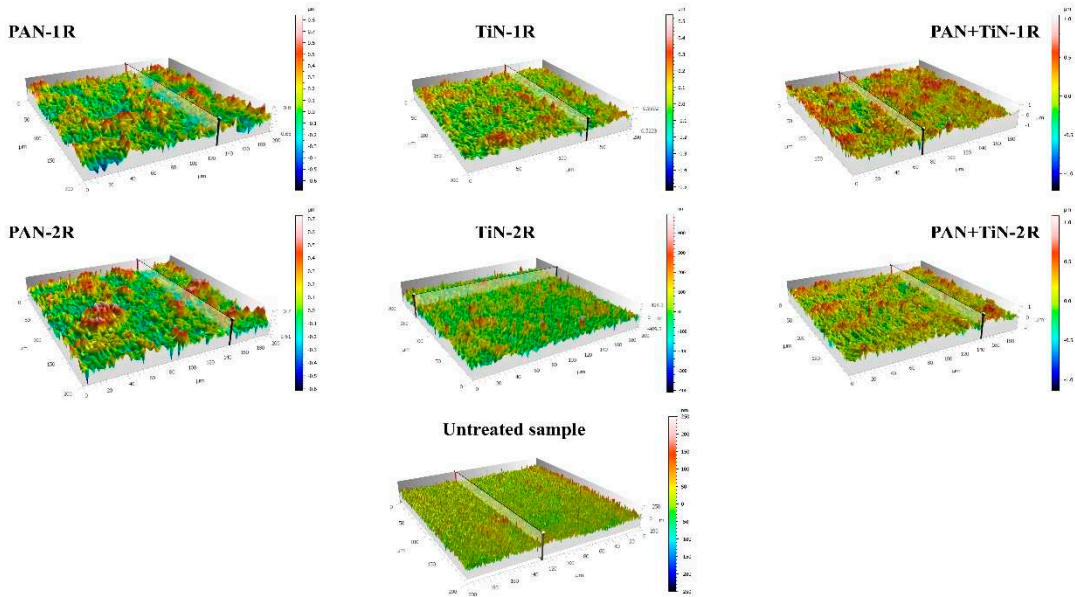
**Table 2.** extracted roughness data from samples showed in Figure 2.

Sample name	Sa* (nm)	Sq** (nm)	Sz*** (nm)	Ra (nm)	Rq (nm)	Rz (nm)
Untreated 1.2379	28.01	36.61	528.9	8.786	11.56	61.80
PAN-1R	156.8	199	1522	60.41	75.23	286.7
PAN-2R	149.7	192.4	1337	49.60	61.88	227.0
PAN+TiN-1R	211	271.8	2261	92.31	118.5	580.3
PAN+TiN-2R	169.5	225.9	2223	58.01	77.66	369.1
TiN-1R	75.4	101.9	1061	27.17	36.49	150.9
TiN-2R	60.92	84.02	903.2	22.18	27.75	126.4

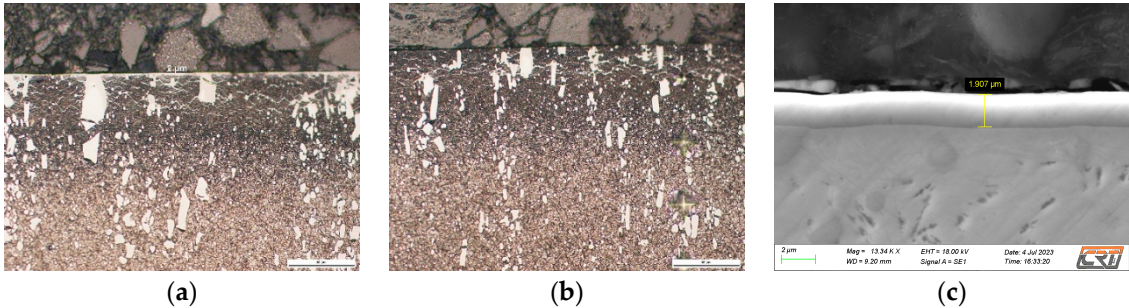
\* Sa: Arithmetic mean deviation. \*\* Sq: Root-mean-square (RMS) deviation of the surface. \*\*\* Sz: Ten point height of the surface.

Analyzing the profilometry data further reveals that only TiN coatings exhibit a doubling of the surface roughness, which can be attributed to the columnar growth of PVD coatings, especially Arc PVD, which introduces additional droplets and coating defects.

Additionally, line scan roughness parameters, including average roughness (Ra), root mean square roughness (Rq), and the difference between the highest peak and the lowest valley on the surface (Rz), are reported in Table 2. Although these parameters are commonly reported in the literature, it is evident that reporting surface roughness in its entirety provides a more precise characterization.



**Figure 1.** Top view profilometry of treated and untreated samples.





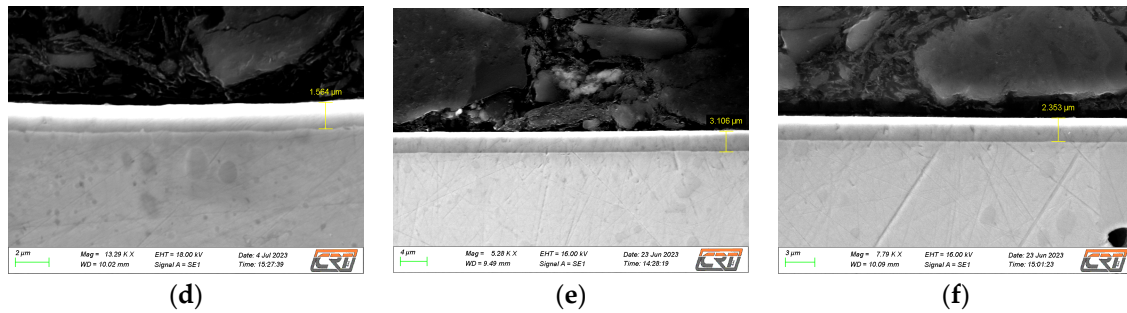


**Figure 2.** OM images of (a) PAN-1R (b) PAN-2R and SEM micrographs of (c) PAN+TiN-1R (d) PAN+TiN-2R (e) TiN-1R (f) TiN-2R.

Figure 2 presents optical and SEM micrographs of cross-sections of the nitrided, nitrided & TiN coated, and only TiN coated specimens with one and two-fold rotation. The measured thickness of the treated samples is provided in Table 3. From Figure 1(a) and (b), it is evident that a white layer (WL) of approximately 2  $\mu\text{m}$  forms only on the one-fold rotation, likely due to increased exposure in the plasma column and higher localized temperature. The nitrogen depth profiles in both samples are similar. The presence of the WL has both positive and negative effects. On one hand, the WL, being hard, compact, composed of ultrafine grains, and resistant, enhances tribo-corrosion properties [9]. On the other hand, it is fragile and susceptible to cracking, fracturing, and delamination in some areas [10]. Previous studies have reported the negative impact of white layers on the adhesion of PVD coatings to substrates, although this is closely related to the method of its formation [11]. The influence of this layer on the adhesion properties of the TiN coating will be discussed later.

**Table 3.** Extracted data from mechanical tests of samples.

Sample name	Treated Thickness ( $\mu\text{m}$ )	Hardness (GPa) at 50mN	Elastic Modulus (GPa) at 50mN	H/E	H <sup>3</sup> /E <sup>2</sup> (GPa)	COF <sup>1</sup>	Scratch Hardness (GPa) at 20N	LC3 <sup>2</sup> (N)
Untreated 1.2379	-	7.37 $\pm$ 0.04	230 $\pm$ 23	0.028	0.0075	0.099 $\pm$ 0.001	5.5 $\pm$ 0.3	-
PAN-1R <sup>3</sup>	60 $\pm$ 5	13.46 $\pm$ 0.69	208 $\pm$ 14	0.065	0.056	0.090 $\pm$ 0.005	17.6 $\pm$ 0.4	-
PAN-2R <sup>4</sup>	65 $\pm$ 5	13.35 $\pm$ 0.2	204 $\pm$ 8	0.065	0.057	0.095 $\pm$ 0.005	18.1 $\pm$ 0.5	-
PAN+TiN-1R	1.9 $\pm$ 0.1	27.62 $\pm$ 0.34	384 $\pm$ 12	0.072	0.143	0.111 $\pm$ 0.015	22.7 $\pm$ 0.4	30 $\pm$ 2
PAN+TiN-2R	1.5 $\pm$ 0.1	27.86 $\pm$ 0.36	366 $\pm$ 9	0.076	0.161	0.115 $\pm$ 0.009	23.8 $\pm$ 0.2	34 $\pm$ 1
TiN-1R	3.0 $\pm$ 0.1	27.41 $\pm$ 0.75	467 $\pm$ 25	0.059	0.094	0.123 $\pm$ 0.002	12.2 $\pm$ 0.2	25 $\pm$ 1
TiN-2R	2.4 $\pm$ 0.1	26.76 $\pm$ 0.33	422 $\pm$ 5	0.063	0.107	0.116 $\pm$ 0.005	10.1 $\pm$ 0.3	18 $\pm$ 1

1. COF: Coefficient of Friction against a 3mm diameter 316L SS ball at a load of 5N. 2. LC3: Critical load for full detachment by micro conical diamond tip of 100 $\mu\text{m}$ . 3. 1R: One-fold rotation. 4. 2R: Two-fold rotation.

Figure 2(c) to (f) reveal that the TiN coatings exhibit a very dense, most likely columnar structure, uniformity, and few defects. As expected, the one-fold rotation generally results in a greater coating thickness than the two-fold rotation. The absence of droplets in these images does not imply the absence of droplets throughout the entire coating. It is claimed that our new advanced PVD machines minimize droplet formation. These droplets play a vital role in determining the final mechanical and corrosion properties of the coatings.

The elasto-plastic properties of the samples were evaluated using nano-indentation and micro scratch tests. The untreated sample exhibits high hardness due to its elevated carbon content. The

addition of approximately 12% chromium makes it suitable for further hardening through nitriding, resulting in an increase of about 1.8 times its original hardness.

Comparing the hardness values of PAN+TiN coatings with only TiN coated samples, it is evident that the final layer hardnesses are quite similar. This can be attributed to the application of a very low load of only 50 mN during nano-indentation. The influence of rotation fold on the results appears to be minimal, and the texture of the coatings does not significantly affect the hardness outcomes.

However, the elastic modulus seems to be affected by PAN treatment as well as the rotation fold. In general, PAN treatment and two-fold rotation demonstrate lower elastic modulus compared to PAN+TiN and TiN coatings with one-fold rotation. The one-fold rotation allows more exposure time to the cathode targets, resulting in a higher impact angle for the ions reaching the surface. This leads to stronger bonding between the coating and the substrate and higher level of stress in the coating, thereby exhibiting higher elastic modulus.

Other factors that influence the elastic modulus include the presence of defects and mismatches between layers. These factors could explain the reduced elastic modulus observed in PAN-treated samples, which persists even after the subsequent TiN coating in PAN+TiN coatings.

Hard coatings, predominantly composed of ceramic materials, find wide application in wear protection. While hardness is commonly associated with wear resistance, it is acknowledged that other factors such as coating elasticity and toughness are equally, if not more, important in scenarios involving abrasion, impact, and erosive wear. Evaluating coating properties solely based on hardness may not provide a comprehensive understanding. Instead, considering ratios such as  $H/E$  and  $H^3/E^2$  can offer valuable insights [12]. A higher  $H/E$  ratio indicates greater resistance to elastic strain failure, signifying better wear resistance. Additionally, coatings with larger  $H^3/E^2$  values are less prone to plastic deformation, indicating higher toughness [12,13].

The calculated  $H/E$  and  $H^3/E^2$  ratios presented in Table 3 indicate significantly low values for the untreated sample, suggesting poor wear properties and toughness. However, after PAN treatment, an improvement in these ratios is observed. The PAN+TiN coatings exhibit the highest  $H/E$  ratio, indicating enhanced wear resistance, along with higher  $H^3/E^2$  values. Generally, PAN treatment prior to coating enhances the wear behavior and toughness of TiN coatings.

The coefficient of friction (COF) plays a crucial role in material selection and determining surface requirements. Table 3 provides COF values for various coatings against a 3mm diameter 316L SS ball under a constant load of 5N. This load level is chosen to ensure minimal surface damage. Based on the findings, the untreated material and PAN-treated samples exhibit the lowest COF, while PAN+TiN and TiN coatings show similar values. This demonstrates that the COF is primarily dependent on the outer layer when the applied force remains within levels that do not damage the surface.

To gain further insight into the behavior of the coefficient of friction (COF), a gradual increase in load was applied to the samples, ranging from 0 to 45N, with a spherical tip of 100  $\mu\text{m}$  in diameter. The objective was to examine how the COF evolved with increasing load. The observed rise in the friction coefficient with the augmentation of the normal load can be attributed to an enhancement in adhesion strength. In many combinations of metal surfaces, the friction coefficient typically starts at a low value when the load is light and then undergoes a transition to a higher value as the normal load is increased. At lower loads, there is minimal or no direct contact between the metallic surfaces, resulting in a low friction coefficient. However, under higher load conditions, the protective film or layer breaks down, leading to intimate metallic contact, which contributes to the observed higher friction [14].

In the initial stages, all samples exhibit relatively similar COF values, except for the untreated sample, which shows a slightly higher COF from the beginning. At approximately 0.2 mm position (equivalent to 6N load, not shown in the graph), the untreated sample also displays a slight reduction in COF, likely due to a decrease in roughness resulting from the breaking down of surface peaks. From this point onwards, the TiN coated samples demonstrate a gradual increase in COF as the load increases until reaching 0.5 mm (15N). Beyond this point, a sharp increase in COF is observed for the

TiN coating, surpassing even the COF of the untreated sample. This behavior may be attributed to the detachment of the TiN coating and its influence on the subsequent path.

On the other hand, the PAN treated samples exhibit a more stable COF until approximately 0.9 mm (27N), after which it starts to rise rapidly. This behavior could be attributed to the participation of detached particles and, most likely, their oxidation. The situation is even more favorable for the PAN+TiN treated samples, as their rapid COF increases occur at around 1 mm (30N). From the results, it can be concluded that COF is not solely dependent on coating thickness, as the TiN-1R sample with a higher thickness compared to the TiN-2R sample exhibits similar behaviors. Meanwhile, the PAN+TiN samples with lesser thicknesses demonstrate the lowest COF values.

Upon examining the penetration depth of the samples in Figure 3, it becomes apparent that the depths are relatively similar among all samples and show minimal dependence on the type of treatment applied.

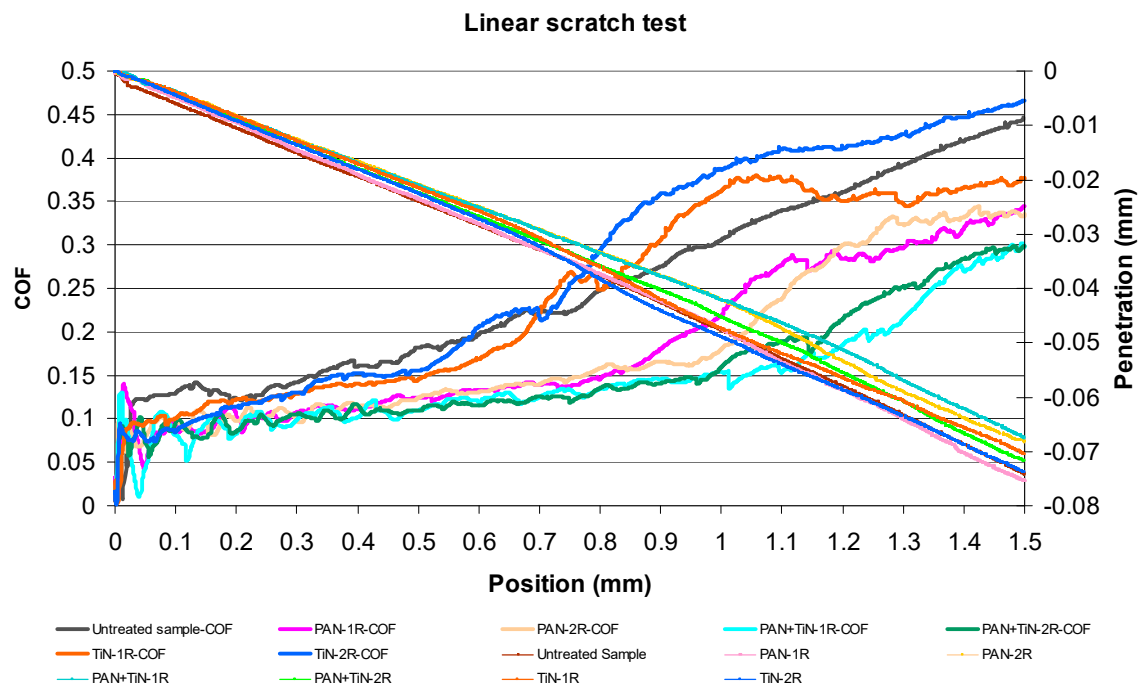


**Figure 3.** COF and penetration depth of 100  $\mu$ m point over a 1.5 mm tracking length position.

In addition to the penetration depth analysis, the scratch test was utilized to gain further insights into the mechanical behavior of the samples. Figure 4 illustrates the scratch tracks of the samples, accompanied by extracted data such as scratch hardness and detachment critical loads (LC3), which are reported in Table 3. By observing the scratch tracks, it is evident that the PAN and PAN+TiN tracks are thinner compared to the others, indicating higher scratch hardness. The data obtained at a normal load of 20N was specifically selected to obtain more precise information, as at this load, cracks have not yet propagated, and no serious delamination or detachment has occurred except for TiN-2R. Notably, PAN+TiN coatings exhibit more than twice the scratch hardness of TiN coatings, showcasing superior performance.

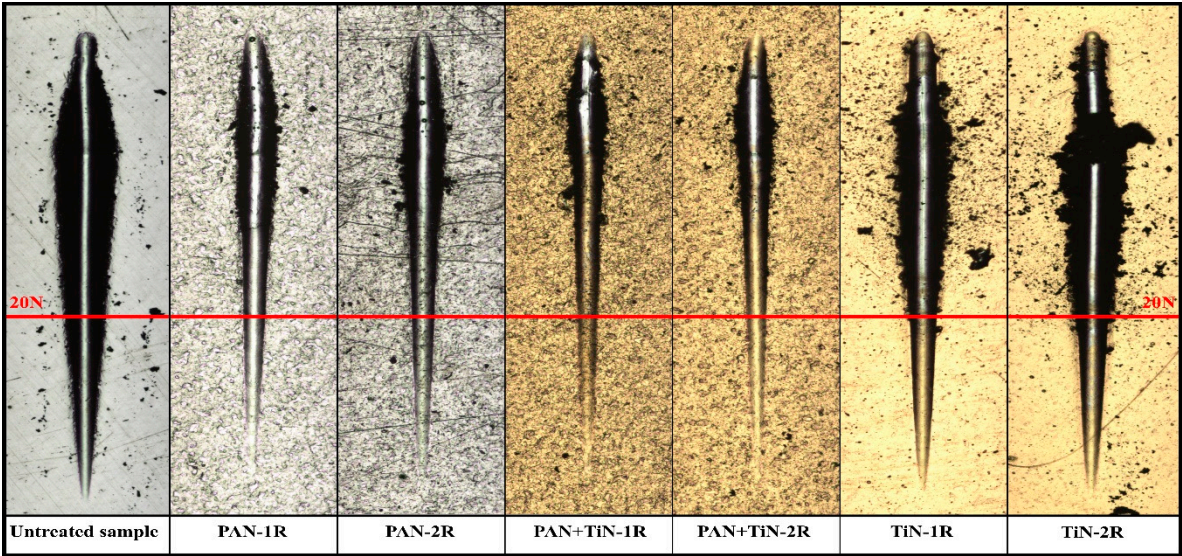


**Figure 4.** Microscratch tracks of various samples from 0 to 45N load with a tip radius of 0.1 mm: untreated sample, PAN-1R, PAN-2R, PAN+TiN-1R, PAN+TiN-2R, TiN-1R, TiN-2R.

Furthermore, a closer examination of Figure 4 draws attention to the initiation points of detachment for TiN coatings, which occur lower loads compared to PAN+TiN coatings, despite their thicker nature. This clearly demonstrates the effectiveness of the previous PAN treatment in improving the scratch hardness of TiN coatings. The measured detachment critical loads of LC3 further confirm this effectiveness.

Tafel tests were conducted to explore the impact of different treatments on the corrosion resistance of the samples. The Tafel graphs in Figure 5 depict the results for the one-fold rotation samples, as the two-fold rotation samples displayed similar behavior. Among all treatments, PAN+TiN exhibits a noteworthy reduction in corrosion current density at the highest open circuit potential (OCP). It appears that TiN coating alone is insufficient to protect the substrate due to the well-known defects commonly found in arc PVD coatings. However, the PAN treatment, by obstructing the diffusion paths of the corrosive solution, provides improved corrosion protection, even though the thickness of the TiN layer in the PAN+TiN treatment is less than that of the sole TiN coatings.

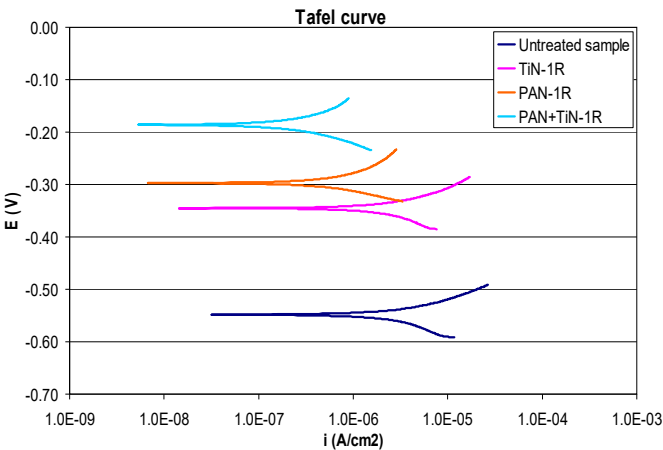


**Figure 5.** Tafel graphs of untreated, PAN-1R, TiN-1R and PAN+TiN-1R samples.

The extracted data is documented in Table 4. The order of reduction in corrosion current densities, along with increasing OCP, is as follows: untreated sample < TiN < PAN < PAN+TiN. Although the treated samples exhibit lower corrosion current densities compared to the untreated one, the examination of their corroded surfaces reveals a localized corrosion behavior. This



observation highlights the significant role of defects, such as droplets, cavities, and micro-cracks, in influencing the corrosion behavior of these samples.

**Table 4.** Corrosion data of samples in 0.5%NaCl solution at room temperature.

Sample name	Current density (nA/cm <sup>2</sup> )	OCP vs. Ag/AgCl (mV)
Untreated 1.2379	6020±800	-548±20
PAN-1R	1460±550	-297±19
PAN+TiN-1R	577±100	-186±24
TiN-1R	4000±120	-345±15

PAN treatment in combination with TiN coatings proved to be a highly effective approach for enhancing the wear resistance and corrosion protection of the TiN coatings. PAN treatment supported TiN coatings by keeping high hardness and reducing elastic modulus, leading to higher ratios of H/E and H<sup>3</sup>/E<sup>2</sup>, enhanced scratch hardness and wear resistance of the TiN coatings.

Overall, the study demonstrates the potential of PAN treatment as a pre-surface modification technique to overcome the limitations of TiN coatings, providing better elasto-plastic and even corrosion properties, while also offering time, energy, and cost savings due to its integration within PVD machines. These findings contribute to the development of more reliable and durable Ti-based coatings, benefiting various industries, including injection molds, punches, dies, and cutting tools.

**Acknowledgments:** Acknowledgements: We sincerely thank CRT Company and its managers for their invaluable support. We also express our gratitude to Prof. S. Trasatti from the University of Milan for his guidance and contributions. We acknowledge the support of all individuals involved that made this research possible.

## References

1. D. Lopez, C. Sanchez, A. Toro, "Corrosion-erosion behaviour of TiN-coated stainless steels in aqueous slurries", *Wear*, 258 (2005), pp. 684-692. <https://doi.org/10.1016/j.wear.2004.09.015>
2. H.W. Wang, M. M. Stack, "Corrosion of PVD TiN coatings under simultaneous erosion in sodium carbonate/bicarbonate buffered slurries", *Surface Coating Technology*, 105 (1998), pp. 141-146. [https://doi.org/10.1016/S0257-8972\(98\)00471-X](https://doi.org/10.1016/S0257-8972(98)00471-X)
3. S. A. Naghibi, K. Raeissi, M.H. Fathi, "Corrosion and tribocorrosion behavior of Ti/TiN PVD coating on 316L stainless steel substrate in Ringer's solution", *Materials Chemistry and Physics*, Volume 148, Issue 3, 2014, Pages 614-623. <https://doi.org/10.1016/j.matchemphys.2014.08.025>
4. R. Ali, M. Sebastiani, E. Bemporad, "Influence of Ti-TiN multilayer PVD-coatings design on residual stresses and adhesion", *Materials & Design* Volume 75, 15 June 2015, Pages 47-56. <https://doi.org/10.1016/j.matdes.2015.03.007>
5. M. Van Stappen, M. Kerkhofs, C. Qaeyhaegens, L. Stals, "Introduction in industry of duplex treatment consisting of plasma nitriding and PVD of TiN", *Wear* 153 (1992) 655-661. [https://doi.org/10.1016/0257-8972\(93\)90314-E](https://doi.org/10.1016/0257-8972(93)90314-E)
6. A.E. Zeghni, M.S.J. Hashmi, "The effect of coating and nitriding on the wear behaviour of tool steels", *Journal of Materials Processing Technology* 155-156 (2004) 1918-1922. <https://doi.org/10.1016/j.jmatprotec.2004.04.281>
7. Y. Sun, T. Bell, "The role of oxidation in the wear of plasma nitrided and PVD TiN coated steel", *Wear* 166 (1993) 119. [https://doi.org/10.1016/0043-1648\(93\)90286-U](https://doi.org/10.1016/0043-1648(93)90286-U)
8. K. Hock, H.J. Spies, B. Larich, G. Leonhardt, "Wear resistance of prenitrided hard coated steels for tools and machine components", *Surface Coating Technology* 88 (1996) 44-49. [https://doi.org/10.1016/S0257-8972\(96\)02914-3](https://doi.org/10.1016/S0257-8972(96)02914-3)
9. D. H. Cho, S. A. Lee, Y. Z. Lee, "Mechanical properties and wear behaviour of the white layer", *Tribology Letter* 45 (2012) 123 - 129. <https://doi.org/10.1007/s11249-011-9869-4>
10. V. Javaheri, S. Sadeghpour, P. Karjalainen, M. Lindroos, O. Haiko, N. Sarmadi, S. Pallaspuuro, K. Valtonen, F. Pahlevani, A. Laukkanen, J. Komi, "Formation of nanostructured surface layer, the white layer, through

- solid particles impingement during slurry erosion in a martensitic medium-carbon steel”, *Wear*, 496–497(2022), 204301. <https://doi.org/10.1016/j.wear.2022.204301>
11. J. Palmers, M. Van Stappen, J. D'Haen, M. D'Olieslaeger, L.M. Stals, G. Uhlig, M. Foller, E. Haberling, “Influence of the presence of white layers formed during grinding and wire-electro-discharge machining on PVD TiN coating adhesion”, *Surface and Coatings Technology* 74-75 (1995) 162-167. [https://doi.org/10.1016/0257-8972\(95\)08226-3](https://doi.org/10.1016/0257-8972(95)08226-3)
  12. A. Leyland, A. Matthews, “On the significance of the H/E ratio in wear control: a nanocomposite coating approach to optimised tribological behaviour”, *Wear* 246 (2000) 1–11. [https://doi.org/10.1016/S0043-1648\(00\)00488-9](https://doi.org/10.1016/S0043-1648(00)00488-9)
  13. X. Chen, Y. Du, Yip-W. Chung, “Commentary on using H/E and H<sup>3</sup>/E<sup>2</sup> as proxies for fracture toughness of hard coatings”, *Thin Solid Films*, 688, 31 (2019), 137265. <https://doi.org/10.1016/j.tsf.2019.04.040>
  14. D. M. Nuruzzaman, M. A. Chowdhury, “Effect of Load and Sliding Velocity on Friction Coefficient of Aluminum Sliding Against Different Pin Materials”, *American Journal of Materials Science*, 2-1 (2012), 26-31. <https://doi:10.5923/j.materials.20120201.05>

**Disclaimer/Publisher’s Note:** The statements, opinions and data contained in all publications are solely those of the individual author(s) and contributor(s) and not of MDPI and/or the editor(s). MDPI and/or the editor(s) disclaim responsibility for any injury to people or property resulting from any ideas, methods, instructions or products referred to in the content.